Electromagnetic coupling reduction in dual-band microstrip antenna array using ultra-compact single-negative electric metamaterials for MIMO application*

Xiao-Long Fu(付孝龙), Guo-Cheng Wu(吴国成)†, Wei-Xiong Bai(白渭雄), Guang-Ming Wang(王光明), and Jian-Gang Liang(梁建刚)

Air and Missile Defense College, Air Force Engineering University, Xi'an 710051, *China*

(Received 2 September 2016; revised manuscript received 4 October 2016; published online 20 December 2016)

In this paper, an ultra-compact single negative (SNG) electric waveguided metamaterial (WG-MTM) is first investigated and used to reduce the mutual coupling in *E* & *H* planes of a dual-band microstrip antenna array. The proposed SNG electric WG-MTM unit cell is designed by etching two different symmetrical spiral lines on the ground, and has two stopbands operating at 1.86 GHz and 2.40 GHz. The circuit size is very compact, which is only $\lambda_0/33.6 \times \lambda_0/15.1$ (where λ_0 is the wavelength at 1.86 GHz in free space). Taking advantage of the dual-stopband property of the proposed SNG electric WG-MTM, a dual-band microstrip antenna array operating at 1.86 GHz and 2.40 GHz with very low mutual coupling is designed by embedding a cross shaped array of the proposed SNG electric WG-MTM. The measured and simulated results of the designed dual-band antenna array are in good agreement with each other, indicating that the mutual coupling of the fabricated dual-band antenna array realizes 9.8/11.1 dB reductions in the *H* plane, 8.5/7.9 dB reductions in the *E* plane at 1.86 GHz and 2.40 GHz, respectively. Besides, the distance of the antenna elements in the array is only $0.35\lambda_0$ (where λ_0 is the wavelength at 1.86 GHz in free space). The proposed strategy is used for the first time to reduce the mutual coupling in *E* & *H* planes of the dual-band microstrip antenna array by using ultra-compact SNG electric WG-MTM.

Keywords: waveguided metamaterial (WG-MTM), dual-band microstrip antenna array, mutual coupling reduction, ultra-compact circuit size

PACS: 41.20.Jb, 73.20.Mf **DOI:** 10.1088/1674-1056/26/2/024101

1. Introduction

Electromagnetic metamaterials (EM-MTMs) have aroused a great deal of interest in physics and engineering applications in recent years due to their various abnormal electromagnetic characteristics that do not occur in nature. Left-handed (LH) MTMs were studied at the beginning of the EM-MTM researches.[1–3] Since the EM-MTMs were proposed, analyzed and experimentally realized,[4–6] a lot of effective and explosive work has been done and the abnormal characteristics of EM-MTMs have been brought into engineering applications such as antennas,[7–10] absorbers,[11–14] cloaking,[15] and many other relevant devices.[16–23] Waveguided metamaterial (WG-MTM) is a category of EM-MTMs, and was first proposed by Yang *et al.* in 2012.[24] In Refs. [25] and [26], the authors proposed a CSRs based SNG electric WG-MTM and a Hilbert-shaped SNG magnetic WG-MTM respectively, and both of them have ultra-compact sizes. Despite these fruitful developments about WG-MTM, there has been reported no structure of WG-MTM with the advantages of ultra-compact size and dual-band.

Electromagnetic mutual coupling reduction of a closely spaced antenna array is an old but very hot and necessary issue of antenna array design. For a conventional antenna array, in order to obtain low mutual coupling and good performances, the distance of antenna elements should be at least $\lambda_0/2$ (where λ_0 is the wavelength at the operating frequency point in free space). In order to reduce the interference coming from the mutual coupling and improve the performances of antenna arrays, several strategies have been devoted to this area, such as EM bandgap structures (EBG),[27,28] frequency-selective surface (FSS),[29] SNG WG-MTMs,[24–26] and the resonant slits or defected ground structure (DGS).[30,31] Although these studies achieved a considerable mutual coupling reduction, they were only for the single band antenna array. For dual/multi-band antenna arrays, the mutual coupling of antenna elements has greater influence on the performances, so dual/multi-band recouplers are necessary and important. In Ref. [32] a T-shape slot impedance transformer has been used as a dual-band recoupler to reduce the mutual coupling of two very closely positioned dual-band PIFAs. According to the property of SNG WG-MTM, we can also use the dual-band SNG WG-MTM to reduce the mutual coupling of dual-band antenna arrays.

In this paper, we first propose a novel ultra-compact dual-band SNG electric WG-MTM. The proposed WG-MTM has two bandgaps with four transmission zeros caused by the neg-

*Project supported by the National Natural Science Foundation of China (Grant No. 61372034).

†Corresponding author. E-mail: wgc805735557@163.com

© 2017 Chinese Physical Society and IOP Publishing Ltd

ative permittivity in the vicinity of electric resonance. The proposed structure has a very compact size due to the spiral lines etched on the ground, which is only 4.8 mm×10.7 mm (equal to $\lambda_0/33.6 \times \lambda_0/15.1$, where λ_0 is the wavelength at 1.86 GHz in free space). Taking advantage of the proposed SNG WG-MTM, we embed a cross shaped array of the proposed WG-MTM into a dual-band microstrip antenna array. The designed antenna array and a conventional one are fabricated and measured. The measured results show that they are in good agreement with the simulations. Compared with the conventional antenna array, the designed one achieves mutual coupling reductions of 9.8/11.1 dB in the H plane and 8.5/7.9 dB in the E plane, at 1.86 GHz and 2.40 GHz, respectively. Besides, the distance between antenna elements in the designed antenna array is only $0.35\lambda_0$.

2. Dual-band ultra-compact SNG electric WG-MTM

The structure of the proposed ultra-compact SNG electric WG-MTM and the simulation setup in Ansoft HFSS are shown in Fig. 1, and the substrates used here are each FR4_epoxy with a permittivity of 4.4, thickness of 1.6 mm and loss tangent of 0.001.

2.1. SNG electric WG-MTM design and simulation setup

As shown in Fig. 1, the structure of the proposed ultra-compact SNG electric WG-MTM is designed by etching two symmetrical spiral lines with different lengths on the ground (referred to as loop 1 and loop 2). The structure dimensions are given as follows: $l_1 = 4.4$ mm, $l_2 = 5.7$ mm, $w_1 = 0.2$ mm, and $w_2 = 0.4$ mm. It is very obvious that the circuit size of the proposed WG-MTM is very compact, which is only 4.8 mm×10.7 mm ($\lambda_0/33.6 \times \lambda_0/15.1$, where λ_0 is the wavelength at 1.86 GHz in free space).

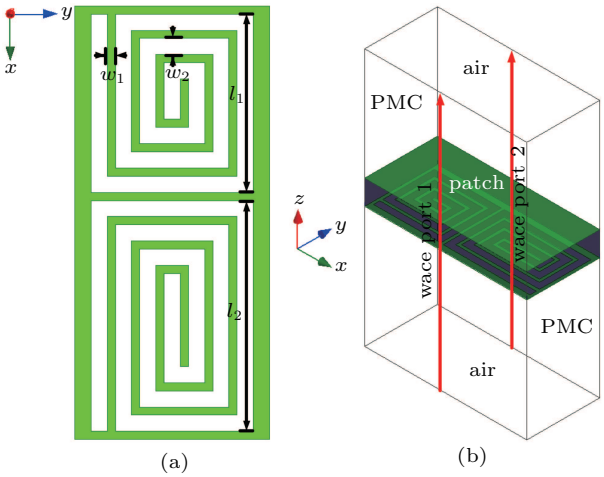


Fig. 1. (color online) (a) Unit cell of the proposed SNG electric WG-MTM and (b) simulation setup in Ansoft HFSS.

For characterization and design, the simulator Ansoft HFSS is employed. In the simulation setup shown in Fig. 1(b), the waveguide is illuminated by a dominant transverse electric and magnetic (TEM) plane wave with the wave vector along the y direction and the electric field (E field) polarized along the z direction. Two wave ports are distributed in the front and on the back side of the proposed structure. The two walls along the x axis are assigned as perfect magnetic conductors (PMC) to mimic an infinite array. Due to the radiation of the proposed structure, a sufficiently larger air box whose bottom surface is set as the radiation boundary is a continuing substrate layer to prevent reflections from the computational domain.

2.2. Simulated results and analysis

The simulated results of the proposed ultra-compact SNG electric WG-MTM are plotted in Fig. 2.

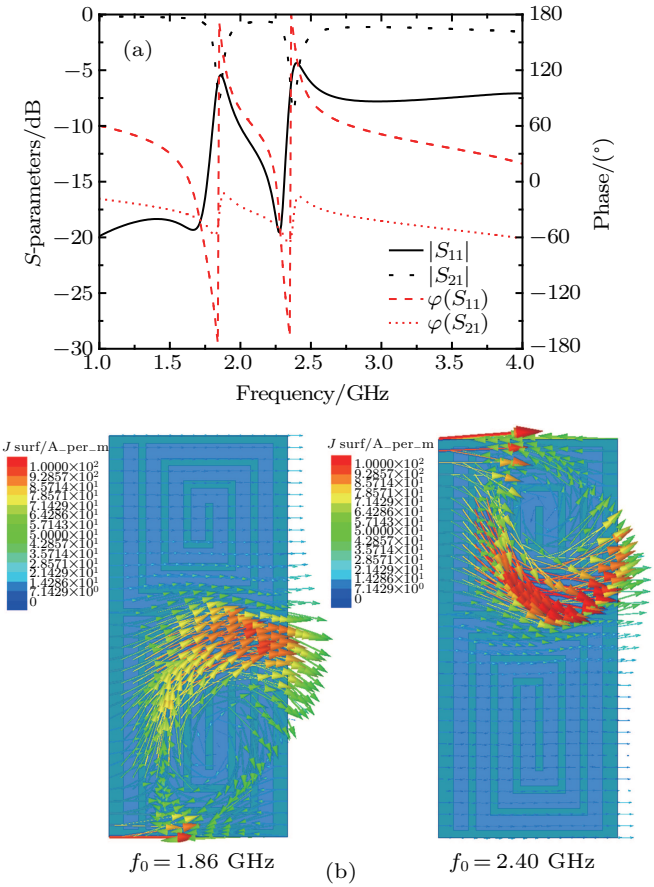


Fig. 2. (color online) Simulated results of the proposed SNG electric WG-MTM, showing (a) S parameters and phase, and (b) surface current vector distribution.

From Fig. 2(a), it can be seen that two obvious stopbands with transmission zeros identified from the transmission dips occurring at 1.86 GHz and 2.40 GHz are clearly observed for the proposed SNG electric WG-MTM. In order to further investigate the causes of stopbands, the surface current vector distributions at 1.86 GHz and 2.40 GHz are given in Fig. 2(b). It is very clear that when the proposed SNG electric WG-MTM operates at 1.86 GHz, the surface current vector is mainly concentrated in the long spiral line loop (loop 2); similarly, when the proposed SNG electric WG-MTM works at

2.40 GHz, the surface current mainly concentrates in the short spiral line loop (loop 1).

According to the electromagnetic performances of the proposed SNG electric WG-MTM, it is very obvious that the two stopbands in the transmission coefficients are attributable to the electric resonance of the developed particle when it impinges to the axial E field of the incoming wave. As a result, the effective permittivity of the proposed metasurface is negative and the effective permeability is positive at the two stopbands, which are indicated in Fig. 3.

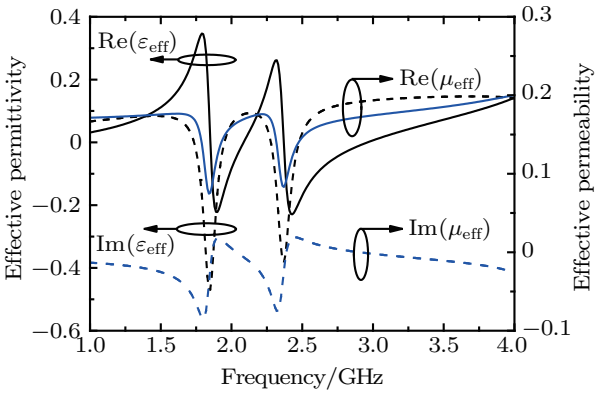


Fig. 3. (color online) Effective permeability and permittivity of the proposed SNG electric WG-MTM.

According to Fig. 3, it can be seen that when the proposed WG-MTM operates around 1.86 GHz and 2.40 GHz, the change trend of the effective permittivity is first to monotonically increase to a maximum and then decreases monotonically to a minimum; after that, the effective permittivity begins to monotonically increase. At the same time, the effective permeability is kept positive. Therefore, this is the reason for the electric resonance at the two stopbands of the proposed SNG electric WG-MTM.

In order to investigate the proposed SNG electric WG-MTM in depth, the influences of loop 1 and loop 2 on the electromagnetic properties are given in Fig. 4. It can be seen that the two stopbands are mainly determined by the lengths of loop 1 and loop 2, respectively.

As shown in Fig. 4(a), it is very obvious that when the length of loop 2 is kept unchanged, with the decrease of the length of loop 1, the second stopband will shift toward high frequency band, while the first stopband is basically kept unchanged. As a comparison, in Fig. 4(b), when the length of loop 1 is kept unchanged, with the decrease of the length of loop 2, the first stopband will shift toward the high frequency band, while the second stopband is basically kept unchanged. Moreover, when the two stopbands shift toward the high frequency band, their bandwidths stay the same. Therefore, the two stopbands of the proposed SNG electric WG-MTM can be controlled by adjusting the lengths of loop 1 and loop 2, independently.

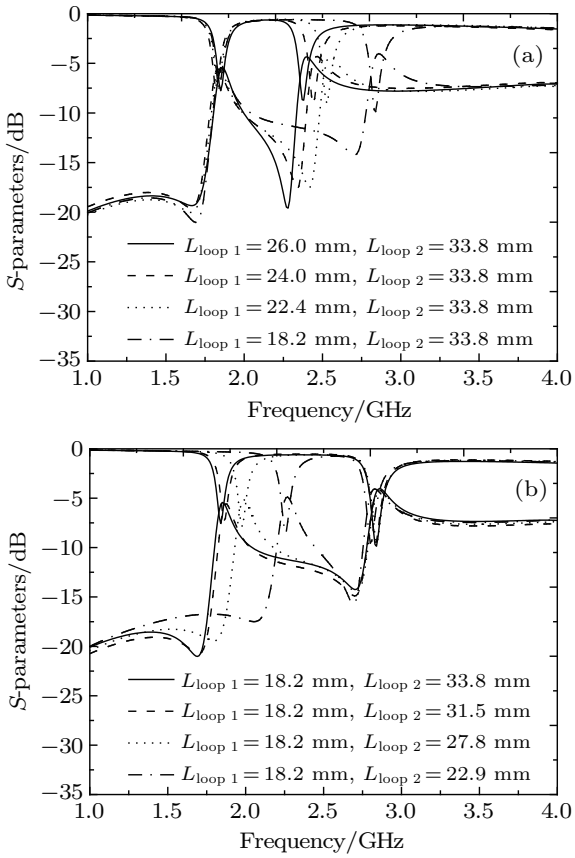


Fig. 4. Influences of (a) loop 1 and (b) loop 2 on the electromagnetic property of the proposed SNG electric WG-MTM.

3. Mutual coupling reduction of dual-band microstrip antenna array

3.1. Theory of mutual coupling reduction

Figure 5 shows the schematic diagram of the mutual coupling reduction of a two-element microstrip antenna array with the proposed SNG electric WG-MTM array.

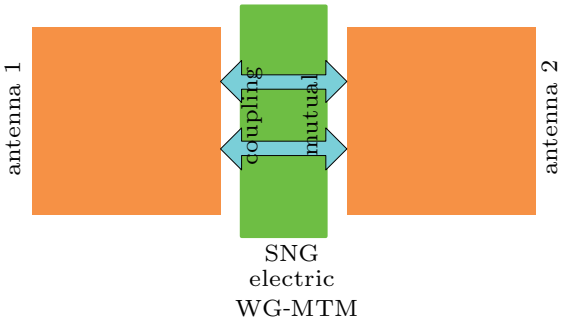


Fig. 5. (color online) Schematic diagram of the mutual coupling reduction.

A two-port microwave network is used to explain the theory of mutual coupling of two microstrip antenna elements in the designed antenna array. In the two-port network, the transmission and reflected signals can be represented by the scattering matrix:

$$\begin{bmatrix} V_1^- \\ V_2^- \end{bmatrix} = \begin{bmatrix} S_{11} & S_{12} \\ S_{21} & S_{22} \end{bmatrix} \begin{bmatrix} V_1^+ \\ V_2^+ \end{bmatrix}. \quad (1)$$

As shown in Eq. (1), V_1 and V_2 are the amplitudes of voltage at the two ports, the '+' and '−' represent the directions of transmission, the S_{ij} $(i \neq j)$ represents the mutual coupling between two antenna elements. Assuming that there is no loss of the antenna array, equation (1) can be simplified into the following equation:

$$\begin{bmatrix} V_1^- \\ V_2^- \end{bmatrix} = \begin{bmatrix} 0 & S_{12} \\ S_{21} & 0 \end{bmatrix} \begin{bmatrix} V_1^+ \\ V_2^+ \end{bmatrix}. \tag{2}$$

According to Eq. (2), the necessary condition for perfect decoupling is $S_{ij} = 0$, $(i \neq j)$, due to this condition, the mutual impedance of the antenna array is $Z_{ij} = 0$, $(i \neq j)$. For the proposed ultra-compact dual-band SNG electric WG-MTM, the effective impedance of the resonance-frequency will be a pure imaginary, and as a result, it can be used to reduce mutual coupling of microstrip antenna arrays.

3.2. Mutual coupling reduction and result discussion

One of the most important applications of the proposed dual-band ultra-compact SNG electric WG-MTM is to suppress mutual coupling of a closely spaced dual-band antenna array at frequencies located in the bandgap regions. In order to test this capability, a 2×2 dual-band microstrip antenna array loaded with a cross shaped array of the proposed dual-band SNG electric WG-MTM and a conventional one are fabricated and measured. Figure 6 gives the structure of the designed dual-band microstrip antenna array, it can be seen that the designed array consists of four dual-band microstrip patch antenna elements and a cross shaped array of the proposed dual-band SNG electric WG-MTM.

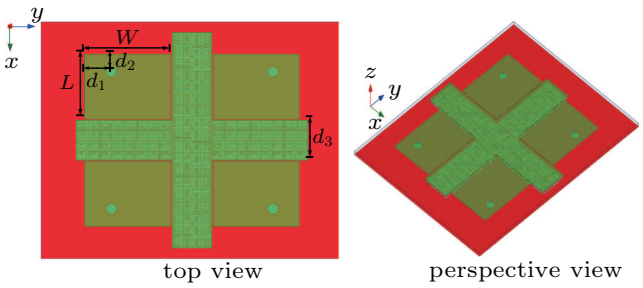


Fig. 6. (color online) Structure of the proposed SNG electric WG-MTM loaded dual-band antenna array.

As shown in Fig. 6, the structure dimensions of the designed dual-band microstrip antenna array are set to be $L = 28.5$ mm, $W = 38$ mm, $d_1 = 11.8$ mm, $d_2 = 7.65$ mm, and $d_3 = 18.6$ mm. Since the operating frequency and signal inhibition level are insensitive to the periodicity once the dual-band SNG electric WG-MTM array is fixed, the distance of the antenna element is mainly dependent on the dimension of the proposed SNG WG-MTM, which is only 56.6 mm ($0.35\lambda_0$, where λ_0 is the wavelength at 1.86 GHz in free space). The photographs of the fabricated dual-band microstrip antenna arrays are shown in Fig. 7.

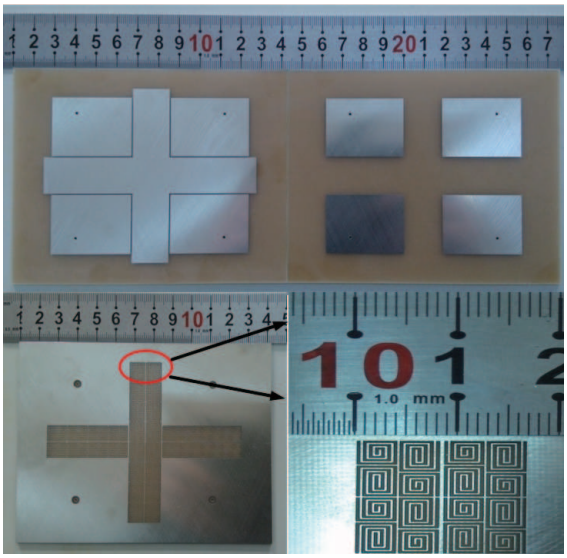


Fig. 7. (color online) Photographs of the designed and conventional dual-band microstrip antenna arrays.

According to Fig. 8, which gives the comparison between the simulated and measured S parameters of the designed and conventional dual-band antenna arrays. The simulated and measured results are in good agreement with each other in all conditions except for a slight frequency shift upwards (with maximum 0.03 GHz) in the measurement, indicating that this design is effective.

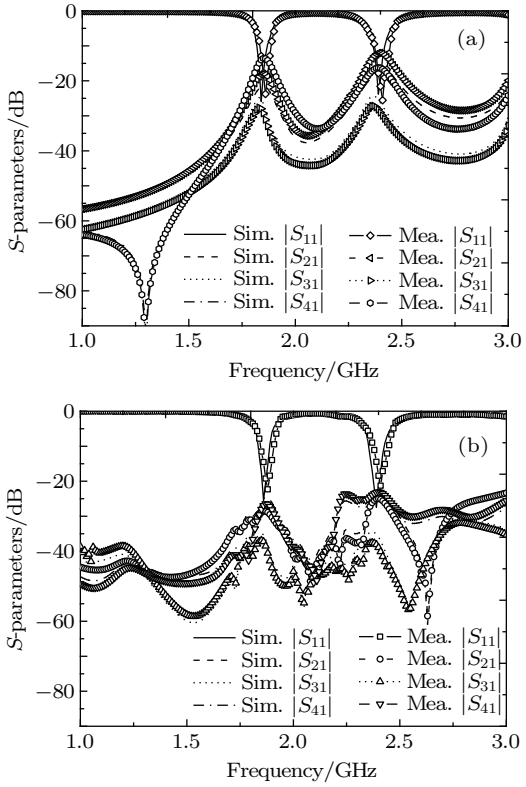


Fig. 8. (color online) Measured and simulated S parameters of the dual-band antenna arrays: (a) the conventional dual-band antenna array and (b) the designed dual-band antenna array.

According to the results shown in Fig. 8, the measured mutual coupling of the conventional dual-band antenna array is 13.6 dB in the H plane and 18.2 dB in the E plane at

1.86 GHz, 12.1 dB in the *H* plane and 16.4 dB in the *E* plane at 2.40 GHz, respectively. While for the designed one, the measured mutual coupling reduces to 23.4 dB in the *H* plane and 26.7 dB in the *E* plane at 1.86 GHz, 23.2 dB in the *H* plane and 24.3 dB in the *E* plane at 2.40 GHz, respectively. Therefore, the mutual coupling realizes 9.8/11.1 dB in the *H* plane and 8.5/7.9 dB in the *E* plane at 1.86 GHz and 2.40 GHz. These reduction levels are very satisfactory for antenna elements with such a close proximity in the single negative electric waveguided metamaterial loaded antenna array.

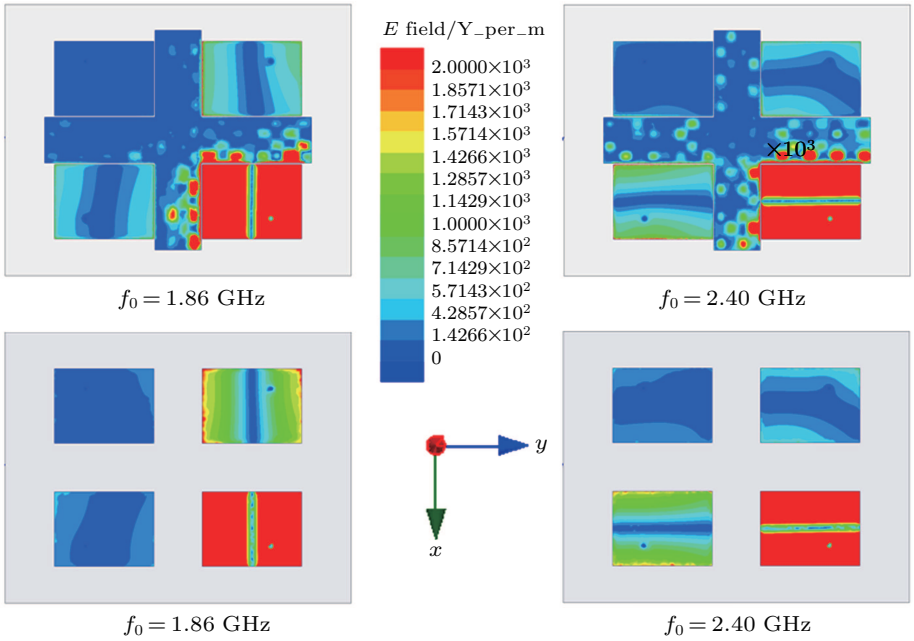


Fig. 9. (color online) Surface current distributions at 1.86 GHz and 2.40 GHz on the top metallic plate of the antenna arrays.

Figure 9 gives the surface current distributions at 1.86 GHz and 2.40 GHz on the top metallic plates of the designed and conventional dual-band antenna arrays. It can be seen that when the two antenna arrays operate at 1.86 GHz, the *H* plane is parallel to the *YOZ* plane and the *E* plane is parallel to the *XOZ* plane, while the *H* plane is parallel to the *XOZ* plane and the *E* plane is parallel to the *YOZ* plane at 2.40 GHz. As shown in Fig. 8, a high consistence of the surface currents is observed in the two antenna arrays at 1.86 GHz and 2.40 GHz. In the conventional dual-band antenna array, there are very strong currents that are coupled from the excited antenna element to the adjacent ones, while in the SNG electric WG-MTM loaded antenna array, the coupling power is mainly trapped and absorbed in the cross shaped MTM array, enabling little transmitted energy in the adjacent antenna elements, which proves that the metasurface array is a good antenna decoupler.

The comparisons of the measured far-field radiation patterns in *E* & *H* planes between the WG-MTM loaded and conventional dual-band antenna arrays at 1.86 GHz and 2.40 GHz are given in Figs. 10(a) and 10(b) respectively. Significantly, the given measured far-field radiation patterns are evaluated under the condition of one-port excitation (element radiation behavior but not array behavior). According to the results, the measured far-field radiation patterns at 1.86 GHz and 2.40 GHz of the WG-MTM loaded and conventional dual-band antenna arrays are in good agreement. Besides, the WG-MTM loaded dual-band antenna array obtains an improved front-to-back ratio of the patterns, namely reducing the back radiation and increasing the front radiation.

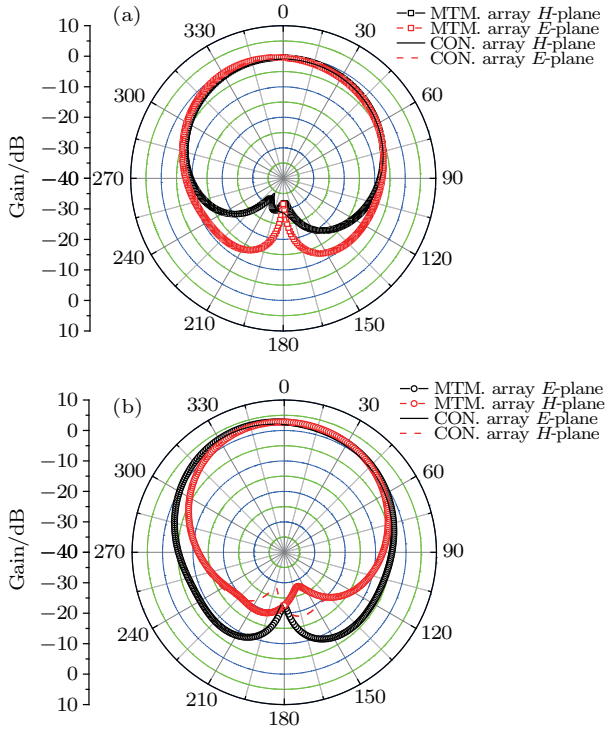


Fig. 10. (color online) Measured far-field radiation patterns of the WG-MTM loaded and conventional dual-band antenna arrays at (a) 1.86 GHz and (b) 2.40 GHz.

4. Conclusions

In this study, we propose an ultra-compact dual-band SNG electric WG-MTM, and use it to reduce the mutual coupling of a 2×2 dual-band microstrip antenna array. The proposed SNG electric WG-MTM is designed by etching two different symmetrical spiral line loops on the ground, and the two stopbands at 1.86 GHz and 2.40 GHz of the proposed WG-MTM are caused by the negative permittivity in the vicinity of electric resonance. Then, a dual-band microstrip antenna array loaded with a cross shaped array of the proposed WG-MTM is designed, fabricated and measured. The measured and simulated results are in good agreement with each other. According to the measured results, it can be seen that compared with the conventional dual-band antenna array, the designed one achieves the mutual coupling reductions of 9.8/11.1 dB in the H plane, 8.5/7.9 dB in the E plane at 1.86 GHz and 2.40 GHz, respectively. Besides, the separated distance between antenna elements in the designed WG-MTM loaded dual-band antenna array is only $0.35\lambda_0$; this method is used for the first time to reduce the mutual coupling in E & H planes of a 2×2 dual-band antenna array by using SNG electric WG-MTM.

Acknowledgment

The authors would like to express their gratitude to China's North Electronic Engineering Research Institute for the fabrications of antenna arrays.

References

[1] Veselago V G 1968 *Sov. Phys. Usp.* **10** 509
[2] Fan Y H, Huang L, Wu S, *et al*. 2015 *Chin. Phys. Lett.* **32** 94101
[3] Peng X, Deng D M, Chen B, *et al*. 2015 *Chin. Phys. B* **24** 124201
[4] Pendry J B, Holden A J, Stewart W J and Youngs I 1996 *Phys. Rev. Lett.* **76** 4773
[5] Pendry J B, Holden A J, Robbins D J and Stewart W J 1999 *IEEE Trans. Microw. Theory Tech.* **47** 2075
[6] Shelby R A, Smith D R and Schultz S 2001 *Science* **292** 77
[7] Wang C, Hu B J and Zhang X Y 2010 *IEEE Anten. Wireless Propag. Lett.* **9** 744
[8] Yuandan D, Toyao H and Itoh T 2011 *IEEE Tran. Anten. Propag.* **59** 4329
[9] Cai T, Wang G M, Zhang X F, Liang J G, Zhuang Y Q, Liu D and Xu H X 2015 *IEEE Tran. Anten. Propag.* **63** 5629
[10] Min Z, Luo J R, He F M, *et al*. 2016 *Chin. Phys. B* **25** 038401
[11] Landy N I, Sajuyigbe S, Mock J J, Smith D R and Padilla W J 2008 *Phys. Rev. Lett.* **100** 207402
[12] Lin B Q, Da X Y, Zhao S H, *et al*. 2014 *Chin. Phys. Lett.* **31** 067801
[13] Jiang Y N, Wang Y, Ge D B, Li S M, *et al*. 2016 *Acta Phys. Sin.* **65** 054101 (in Chinese)
[14] Wang H Y, Zhang X W, Wang H Y, *et al*. 2016 *Chin. Phys. B* **25** 037801
[15] Liu R, Ji C, Mock J J, Chin J Y, Cui T J and Smith D R 2009 *Science* **323** 366
[16] Wu G C, Wang G M, Sun J J, Gao X J and Wang Y W 2014 *Electron. Lett.* **50** 759
[17] Lin, I H, DeVincentis M, Caloz C and Itoh T 2004 *IEEE Trans. Microw. Theory Tech.* **52** 1142
[18] Zeng H Y, Wang G M, Yu Z W, Zhang X K and Li T P 2012 *Radioengineering* **21** 606
[19] Cao W Q, Zhang B N, Yu T B, Liu A J, Zhao S J, Guo D S and Song Z D 2011 *J. Electromagn. Waves Appl.* **25** 1909
[20] Xu H X, Wang G M and Gong J Q 2012 *Chin. Phys. Lett.* **29** 014101
[21] Wu M F, Meng F Y, Wu Q and Wu J 2006 *Acta Phys. Sin.* **55** 5790 (in Chinese)
[22] Xu H X, Wang G M, Wang J F and Yang Z M 2012 *Chin. Phys. B* **21** 124101
[23] Lei Z, Liu X Y and Feng Y J 2016 *Chin. Phys. B* **25** 034101
[24] Yang X M, Liu X G, Zhou X Y and Cui T J 2012 *IEEE Anten. Wireless Propag. Lett.* **11** 389
[25] Xu H X, Wang G M, Qi M Q and Zeng H Y 2012 *Opt. Express* **20** 21968
[26] Xu H X, Wang G M and Qi M Q 2013 *IEEE Trans. Magn.* **49** 1526
[27] Yang F and Rahmat-Samii Y 2003 *IEEE Trans. Antenn. Propag.* **51** 2936
[28] Coulombe M, Farzaneh K S and Caloz C 2010 *IEEE Trans. Antenn. Propag* **58** 1076
[29] Lee D H, Lee Y J, Yeo J, Mittra R and Park W S 2007 *IET Microw. Anten. Propag.* **1** 248
[30] Bait-Suwailam M M, Siddiqui O F and Ramahi O M 2010 *IEEE Anten. Wireless Propag. Lett.* **9** 876
[31] Chiu C Y, Cheng C H, Murch R D and Rowell C R 2007 *IEEE Trans. Antenn. Propag.* **55** 1732
[32] Zhang S, Lau B K, Tan Y, Ying Z N and He S L 2012 *IEEE Trans. Anten. Propag.* **60** 1521